FIRE AND MATERIALS
Fire Mater. 2012; **36**:623–635
Published online 12 October 2011 in Wiley Online Library (wileyonlinelibrary.com). DOI: 10.1002/fam.1123

The new and improved NIST Dragon's LAIR (Lofting and Ignition Research) facility

Samuel L. Manzello[*,†] and Sayaka Suzuki

Fire Research Division, Engineering Laboratory (EL), National Institute of Standards and Technology (NIST), Gaithersburg, MD 20899-8662, USA

SUMMARY

Several studies suggest that the firebrands are a major cause of structural ignition of Wildland–Urban Interface fires in USA and Australia. For 40 years, past firebrand studies have focused on how far firebrands fly and do not assess the vulnerabilities of structures to ignition from firebrand showers. The development of the National Institute of Standards and Technology (NIST) Dragon has allowed the quantification of structure ignition vulnerabilities of full-scale building assemblies. Full-scale tests are necessary to highlight vulnerabilities of structures to ignition under firebrand attack, whereas bench-scale test methods afford the capability to test new firebrand-resistant technologies and may serve as the basis for new standard testing methodologies. To this end, the present investigation was undertaken to construct a new and improved Dragon's Lofting and Ignition Research facility. This entailed removing the NIST Baby Dragon from the wind tunnel facility and inserting the new and improved NIST continuous feed Baby Dragon. The unique feature of the continuous feed Baby Dragon, over the current NIST Baby Dragon, is the capability to produce a constant firebrand shower in order to expose building materials to continual firebrand bombardment. The efficacy of the new experimental facility to determine ignition regime maps of building materials exposed to wind-driven firebrand showers is presented. Specifically, ignition regime maps are presented as a function of continuous firebrand generation rate, wind tunnel speed, and cedar moisture content. Copyright © 2011 John Wiley & Sons, Ltd.

Received 4 May 2011; Revised 6 September 2011; Accepted 7 September 2011

KEY WORDS: Firebrands; WUI Fires; Ignition

1. INTRODUCTION

Wildland–Urban Interface (WUI) fires have caused significant damage to communities throughout the world. Many studies suggest that the firebrands are a major cause of structural ignition of WUI fires in USA and Australia [1–10]. Firebrands are produced as vegetation and structures burn in these fires. To develop scientifically based mitigation strategies to reduce the number of structures lost in these fires, it is necessary to understand the vulnerabilities of structures to firebrand showers. Clearly, firebrands are thought to be important in fire spread. Most of the prior firebrand studies have been focused on how far firebrands fly, known as spotting distance [11–21], and very few studies have examined firebrand generation [22–24] and the ultimate ignition of materials by firebrands [25–29]. As a result, the prior firebrand studies are of limited use to design firebrand-resistant structures.

Manzello *et al*. [30–34] developed an experimental apparatus, known as the National Institute of Standards and Technology Firebrand Generator (NIST Dragon), to investigate ignition vulnerabilities

*Correspondence to: Samuel Manzello, NIST, Gaithersburg, MD 20899-8662, USA. Tel: +1-301-975-6891, Fax: +1-301-975-4052.
[†] E-mail: samuelm@nist.gov

Copyright © 2011 John Wiley & Sons, Ltd.

of structures to firebrand showers. The experimental results generated from the coupling of the NIST Dragon to the Building Research Institute's (BRI) Fire Research Wind Tunnel Facility (FRWTF) have quantified vulnerabilities that structures possess to firebrand showers for the first time. Specifically, the NIST Dragon has been used to determine vulnerabilities of roofing assemblies, building vents, siding treatments, and walls fitted with eaves to firebrand showers. These detailed experimental findings are being considered as a basis for performance-based building standards with the intent of making structures more resistant to firebrand attack.

Full-scale experiments are required to observe the vulnerabilities of structures to firebrand showers, but reduced-scale test methods afford the capability to evaluate firebrand-resistant building elements and may serve as the basis for new standard testing methodologies. To this end, Manzello *et al.* [33,34] developed the NIST Dragon's Lofting and Ignition Research (LAIR) facility to simulate wind-driven firebrand showers at reduced scale. This facility consists of a reduced-scale Firebrand Generator (known as the NIST Baby Dragon) coupled to a bench-scale wind tunnel. The reduced-scale Dragon's LAIR facility was able to reproduce the results obtained from the full-scale experiments conducted pertaining to firebrand penetration through building vents. Specifically, experiments found that firebrands were not quenched by the presence of the mesh and would continue to burn until they were able to fit through the mesh opening, even down to 1.04 mm opening. The experiments demonstrated that mesh was not effective in reducing ignition for the fine fuels tested and that firebrand-resistant vent technologies are needed.

Although the NIST Dragon's LAIR facility and the full-scale NIST Dragon coupled to BRI's FRWTF have been used to expose building elements to firebrand showers, the duration of exposure using the existing apparatus is limited. To develop test methods needed to evaluate different building materials' resistance to firebrand showers requires the capability to generate firebrand showers of varying duration.

Accordingly, the NIST reduced-scale continuous feed Firebrand Generator (the NIST continuous feed Baby Dragon) was developed. The unique feature of the NIST continuous feed Baby Dragon, over the present NIST Dragon, is the ability to produce a constant firebrand shower in order to expose building materials to continual firebrand bombardment. In a very recent study, Suzuki and Manzello [35] characterized the performance of this device. Specifically, the number flux (number of firebrands generated/m^2 s) and the mass flux (mass of firebrands generated/m^2 s) were measured as functions of feeding rate to determine optimum conditions to generate steady firebrand showers. Another key issue is that the firebrand size and mass produced using the NIST continuous feed Baby Dragon (and NIST Dragon) have been tied to those measured from full-scale tree burns and actual WUI fires. Specifically, firebrand sizes produced using this device are commensurate with the characteristics of firebrand exposure at a single location during a severe WUI fire in California that destroyed 254 homes [36]. This is incredibly critical because empirical characterization of firebrand exposure is extremely limited especially with respect to firebrand size distributions during actual WUI fire conditions. Consistently small sizes of windblown firebrands, similar to those generated using this device, were observed by data collection adjacent to a home that survived severe interface fire exposure. This is in stark contrast with the size of firebrands referenced in existing test standards (e.g. ASTM E108 [37]) and wildfire protection building construction recommendations. These arguments were recently expounded in Foote *et al.* [36].

The present investigation was undertaken to construct a new and improved Dragon's LAIR facility. The unique feature of the continuous feed Baby Dragon, over the current NIST Baby Dragon, is the capability to produce a constant firebrand shower in order to expose building materials to continual firebrand bombardment. The main reason to develop the new Dragon's LAIR is to allow detailed study of firebrand ignition of building materials under continual firebrand bombardment. It is desired that the facility may be used to evaluate and compare firebrand-resistant technologies. To this end, the efficacy of this new experimental facility to determine ignition regime maps of building materials exposed to continuous wind-driven firebrand showers is presented.

2. EXPERIMENTAL DESCRIPTION

The experimental apparatus is shown in Figure 1. The description of the NIST reduced-scale continuous feed Baby Dragon has been described in detail elsewhere [35]. However, the device

Copyright © 2011 John Wiley & Sons, Ltd.

DOI: 10.1002/fam

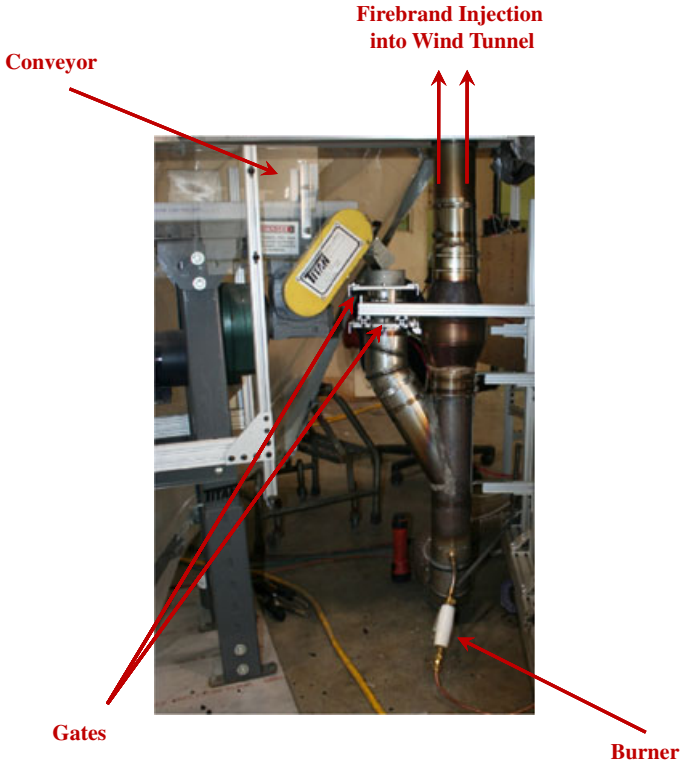

Figure 1. Schematic of NIST continuous feed Baby Dragon (side view).

required considerable redesign to be able to be interfaced with the wind tunnel. Specifically, the gate system needed to be shortened so that the device would fit under the wind tunnel. This version of the NIST reduced-scale continuous feed Baby Dragon consisted of two parts: the main body and the continuous feeding component. The feeding part was connected to the main body and had two gates to prevent fire spread. Each gate was opened and closed alternatively. A blower was connected to the main body.

A conveyer was used to feed wood pieces continuously into the device. The conveyer belt was set at 1.0 cm/s, and groups of wood pieces were put on the conveyer belt at 12.5 cm intervals. In each experiment, the group size placed on the conveyer belt was varied to allow for different firebrand exposures to the target (described below). For all tests, Douglas-fir wood pieces machined with dimensions of 7.9 mm (H) by 7.9 mm (W) by 12.7 mm (L) were used to produce firebrands. The reasons for using wood pieces for these experiments were the following: (1) the use of wood pieces would be easier for other testing laboratories to obtain, and (2) because of the small amount of wood required, it was quite easy to produce these pieces for the reduced-scale tests. These same size wood pieces were used in past studies and have been shown to be commensurate with sizes measured from full-scale burning trees as well as distributions obtained from actual WUI fires [33–36].

An important operational parameter that was varied was the blower speed. When the blower was set to provide an average velocity below 4.4 m/s measured at the exit of the Dragon when no wood pieces were loaded, insufficient air was supplied for combustion and this resulted in a great deal of smoke being generated in addition to firebrands. Above 4.4 m/s, smoke production was mitigated but then the firebrands produced were in a state of flaming combustion as opposed to glowing combustion. It has been suggested that firebrands fall at or near their terminal settling velocity. As such, when firebrands contact ignitable fuel beds, they are most likely in a state of glowing combustion, not open flaming [14]. It is possible for firebrands to remain in a flaming state under an air flow, and it is reasonable to assume that some firebrands may still be in a state of flaming combustion upon impact. The purpose of this device is to simulate firebrand showers observed in long range spotting and therefore glowing firebrands were desired.

Copyright © 2011 John Wiley & Sons, Ltd.

DOI: 10.1002/fam

It is also important to point out that the wood pieces were supported using a mesh with 0.35 mm spacing (see Figure 2 for location). Over the course of the experiments, this mesh was observed to remain usable for 50 experiments. Beyond 50 experiments, holes developed in the mesh as a result of the application of the continuous burner, and therefore the mesh required replacement.

Figure 2 is a schematic of the new and improved NIST Dragon's LAIR facility. The Dragon's LAIR consisted of a reduced-scale continuous feed Firebrand Generator (Baby Dragon) coupled to a reduced-scale wind tunnel. With the exception of the flexible hose, all components of the Baby Dragon were constructed from stainless steel (0.8 mm in thickness).

The test section of the wind tunnel was 50 cm × 50 cm × 200 cm. The flow was provided by an axial fan 91 cm in diameter. Hot wire anemometers were used to quantify the flow distribution, and a calibration was determined as a function of wind tunnel fan frequency.

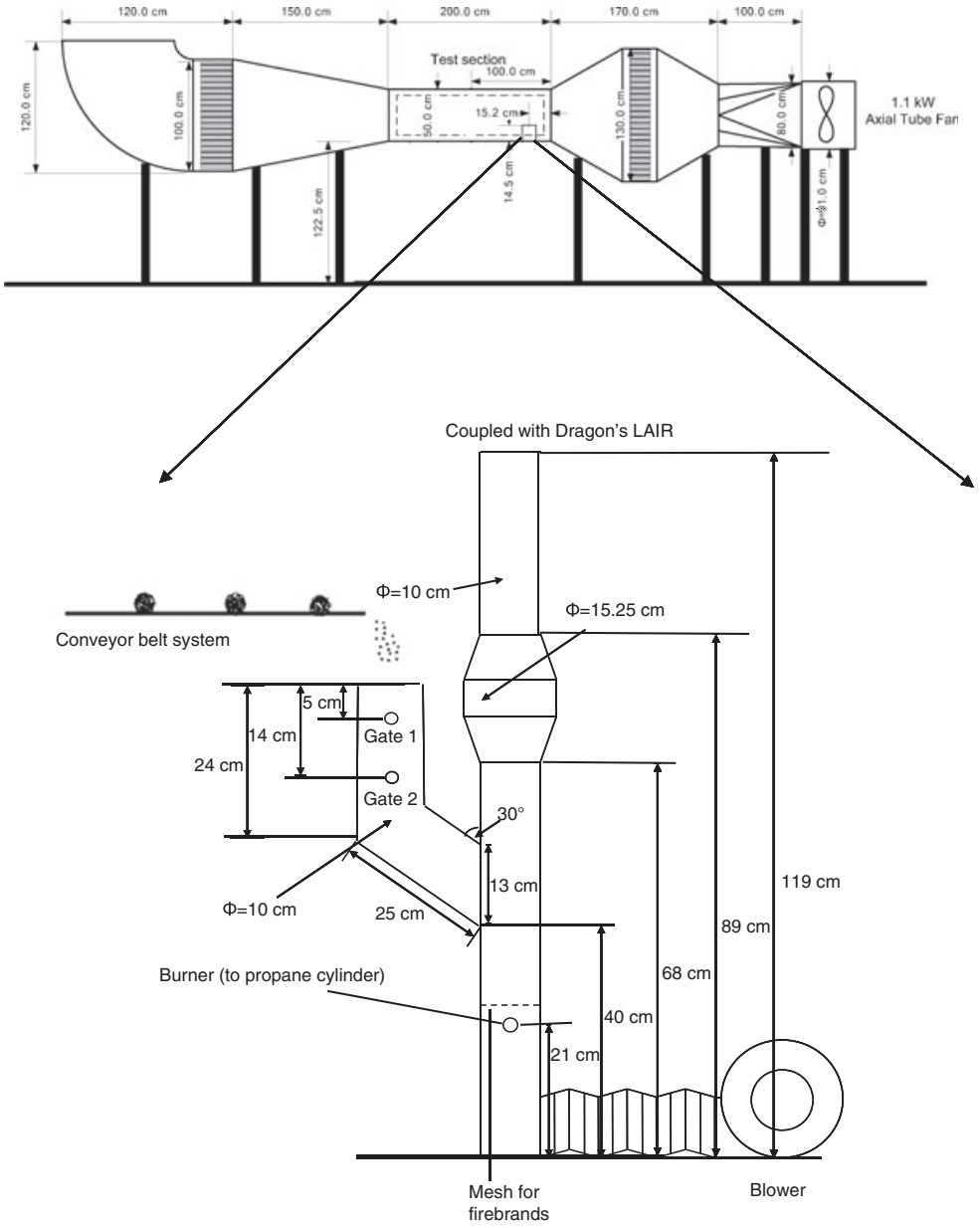

Figure 2. Schematic of the new and improved NIST Dragon's LAIR (Lofting and Ignition Research) facility. The Dragon's LAIR consisted of a reduced-scale continuous feed Firebrand Generator (Baby Dragon) coupled to a reduced-scale wind tunnel.

Copyright © 2011 John Wiley & Sons, Ltd.

DOI: 10.1002/fam

Cedar crevices were constructed for ignition testing. Two pieces of cedar were aligned at an angle of 60°. This angle was selected because consistent ignition behavior has been observed for other building materials ignited by firebrands using this configuration [38]. The dimensions of each cedar piece used were 114 mm wide by 448 mm long. These dimensions were selected because the length covered nearly the entire wind tunnel length and the low width allowed for less flow obstruction. Because the cedar used in these experiments is used for siding, each piece was tapered. Specifically, the largest edge thickness was 11 mm and this tapered down to 3 mm. Because of the arrangement of the crevice, the thick edge of each cedar pieces was offset and this allowed for nominal thickness of 7 mm at the center of the crevice where ignition (described below) was observed. The cedar pieces were held in place using a custom mounting bracket. The location of the cedar crevice was placed about 760 mm from the exit of the mouth of the NIST continuous feed Baby Dragon. This location was selected simply because of the fact that the firebrands were observed to land within the crevice using the wind speed selected in these experiments (6 m/s). The moisture content of the cedar pieces was varied using an oven. Specifically, experiments were conducted using cedar held at 11% moisture content as well as oven dried (placed within the oven held at 104°C for 4 h). Cedar was selected because it is a common material used for both siding and roofing assemblies.

The experiments were conducted in the following manner. The cedar crevice was placed inside the test section, and the door of the test section was then closed. The wind tunnel speed was set to 6 m/s (fixed for all experiments). The blower of the NIST reduced-scale continuous feed Baby Dragon was set at 4.4 m/s, and one propane burner was ignited and inserted into the side of the device. The propane burner was kept on during the entire experiment. The conveyer was then switched on and wood pieces were fed into the stainless-steel pipe first, and then the gate near the conveyer was opened. The gate near the conveyer was then closed, and the other gate was then opened to allow the wood pieces to fall into the Dragon for ignition. Feeding continued for various durations (5 min, 10 min) until ignition was observed. The experiments were recorded using a digital video recorder (30 frames per second) for subsequent analysis (described in the following paragraph).

Five different loadings of wood pieces were used for the ignition studies: 5, 10, 15, 30, and 40 pieces. The mean and the standard deviation of the mass were 2.4 ± 0.2 g for 5 pieces (feed rate of 11.7 g/min), 4.8 ± 0.2 g for 10 pieces (feed rate of 23.1 g/min), 7.2 ± 0.2 g for 15 pieces (feed rate of 34.6 g/min), 14.4 ± 0.1 g for 30 pieces (feed rate of 69.1 g/min), and 19.1 ± 0.2 g for 40 pieces (feed rate of 91.7 g/min), respectively.

3. RESULTS

The number flux, at the exit of the device, was measured as a function of the feed rate. Mass flux data were calculated by multiplying the number flux and the average mass of each firebrand at different feed rates. To measure the firebrand mass, a series of water pans were placed downstream of the NIST reduced-scale continuous feed Baby Dragon after firebrand production reached steady conditions. Water pans were used to quench combustion of the firebrands. If the water pans were not used, the firebrands would continue to burn, and by the time collection was completed only ash would remain.

After the experiment, the pans were collected and the firebrands were filtered from the water using a series of fine mesh filters. Firebrands were dried in an oven, at 104°C, for 4 h. The mass and dimensions of each firebrand were measured using precision calipers (1/100 mm resolution) and a precision balance (0.001 g resolution). The mean mass and standard deviation of each firebrand were similar for all feed rates (e.g. 0.03 ± 0.006 g for 15 pieces, 0.04 ± 0.007 g for 30 pieces).

These analyses were critical to determine the mass generation rate of firebrands for each feed rate. These data are shown in Figure 3. As can be seen, the generation rate (g/s) was linear and increased with an increase in wood feed rate.

Ignition regime maps were determined as a function of feed rate (related to glowing firebrand generation rate; see Figure 3) for fixed wind tunnel speed (6 m/s) and two different cedar crevice moisture contents. Results are shown in Figures 4 and 5. Ignition delay times were measured from the time the first firebrand was deposited inside the crevice to the observation of smoldering ignition (smoldering ignition, defined as intense glowing combustion (smoke production) within the cedar, is shown in Figure 6). In this image, the cedar was oven dried, the wind tunnel speed was 6 m/s, and

Copyright © 2011 John Wiley & Sons, Ltd.

DOI: 10.1002/fam

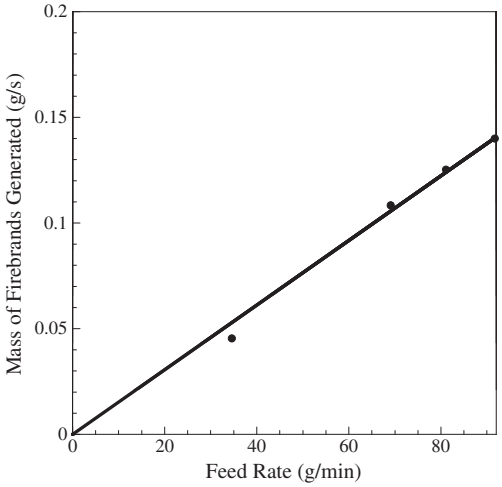

Figure 3. Mass generation rate of firebrands for each feed rate.

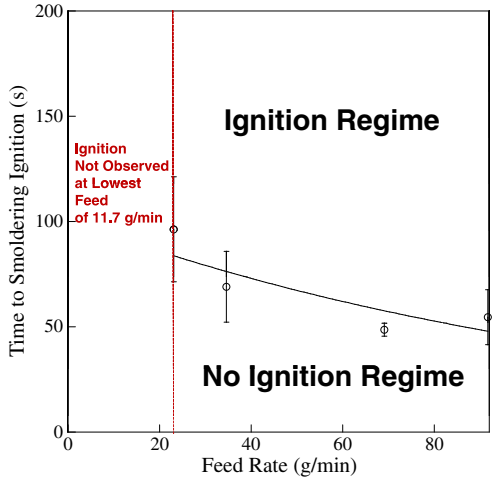

Figure 4. Ignition regime maps (smoldering ignition—SI) as a function of feed rate for fixed wind tunnel speed (6 m/s) when using dried cedar crevices.

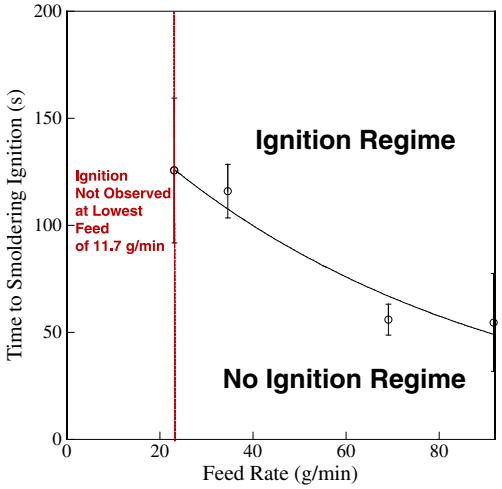

Figure 5. Ignition regime maps (smoldering ignition—SI) as a function of feed rate for fixed wind tunnel speed (6 m/s) when using moist cedar crevices.

Copyright © 2011 John Wiley & Sons, Ltd.

DOI: 10.1002/fam

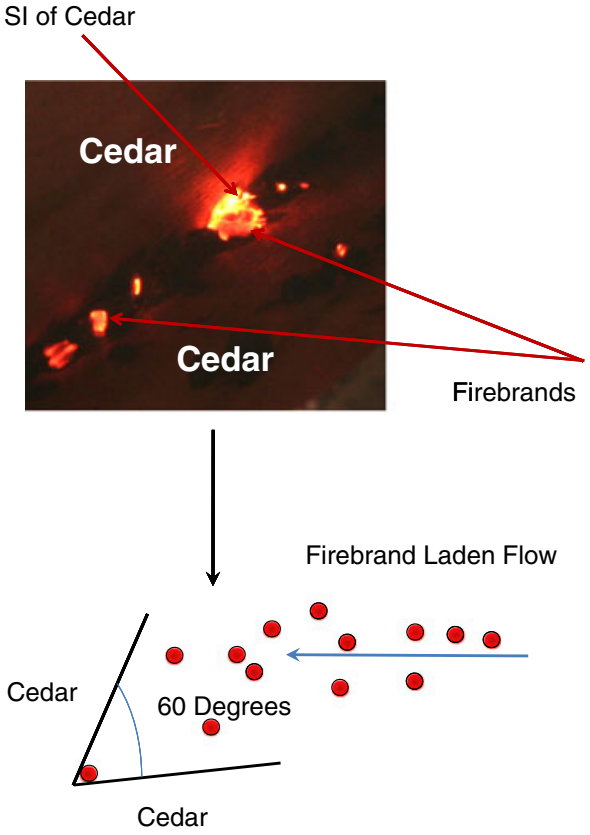

Figure 6. Picture of smoldering ignition of the cedar crevice. In this image, the cedar was oven dried, the wind tunnel speed was 6 m/s, and the firebrand generation rate was 0.03 g/s (based on a feed rate of 23.1 g/min).

the firebrand generation rate was 0.03 g/s (based on a feed rate of 23.1 g/min). Three repeat experiments were performed for each feed rate. Each data point represents the average of three experiments (average ± standard deviation). As can be seen, for a given moisture content and wind speed, the ignition delay time was observed to decrease as the feed rate (corresponding to firebrand generation rate) was increased. For both dried and moist cedar crevices, smoldering ignition was observed for all feeding rates considered with the exception of five pieces.

To explain these results, it is important to consider the heat and mass transfer processes that take place at the fuel bed (cedar in this case) in contact with a glowing firebrand. The deposited firebrands heat up the surface resulting in the production of pyrolysates. As a result, flammable air/fuel mixtures are formed above the cedar crevice. Continued heat supplied from the firebrands contributes to exothermic gas-phase reaction, leading to ignition. The net heat flux, q''_{net}, to the fuel bed from the impinged firebrands is given as (see Figure 7):

$$q''_{\text{net}} = q''_{\text{FB}} - \left(q''_{\text{conv}} + q''_{\text{rad}} + \dot{m}''L_{\text{v}}\right) \tag{1}$$

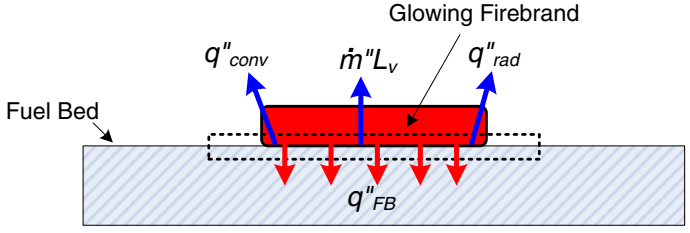

Figure 7. Heat and mass transfer processes that take place at the fuel bed in contact with a glowing firebrand.

Copyright © 2011 John Wiley & Sons, Ltd.

DOI: 10.1002/fam

where q''_{FB} is the heat flux from the firebrands, q''_{conv} is the convective heat flux, q''_{rad} is the radiative heat flux, $\dot{m}''$ is the mass loss rate per unit area, and L_v is the heat of gasification of cedar. The ignition time for thermally thick materials is known to be proportional to the room temperature density, ρ, of the material and inversely proportional to the square of the net heat flux to the fuel bed, q''_{net} [39,40].

$$t_{ig} \propto \frac{\rho}{\dot{q}''^{2}_{net}} \tag{2}$$

As the generation rate of firebrands was increased (from increased feed rate), for a given cedar moisture content and air flow, the resulting firebrand heat flux increased leading to an increase in the net heat flux to the cedar crevice. Specifically, the mechanism by which the firebrand heat flux increased with firebrand generation rate was due to a greater accumulation of firebrands within the crevice itself. At a feeding rate of 11.7 g/min, the firebrand generation rate was insufficient to be able to transfer the necessary heat flux to produce ignition. This is not to say that firebrands did not accumulate in the cedar crevice at a feed rate of 11.7 g/min; rather, intense glowing combustion was not sustained because of the delayed arrival times of firebrands at this low feeding rate (see Figure 8).

As can be seen, the resulting ignition delay time was observed to be higher for cedar crevices held at 11% moisture content when applied to the same firebrand generation rate as the dried cedar crevices. The moisture embedded in the cedar samples reduces the thermal efficiency because the heating and gasification of water consume additional energy. Consequently, this will result in the high value of heat of gasification in Equation 1, reducing the net heat flux to the fuel bed. The moisture content is also known to affect the room temperature density of the fuel bed material, the thermal conductivity, and the heat capacity, and thus the thermal inertia. A high thermal inertia value for a wet fuel bed increases a thermal resistance to changes in temperature, reducing ignitibility.

Under all conditions at a wind tunnel speed of 6 m/s, smoldering ignition was observed to transition to flaming ignition. The time to flaming ignition, after the onset of the first firebrand within the crevice, was also measured and is shown in Figures 9 and 10. A picture of flaming ignition is shown in Figure 11. As compared to the time required to reach smoldering ignition, the time to reach flaming ignition was larger as the feeding rate (corresponding to firebrand generation rate) was decreased. This is clearly seen in the larger standard deviation observed for the lower feed rates.

The transition to flaming ignition from smoldering ignition is a fast exothermic gas-phase reaction and requires two conditions to occur: a mixture of gases and air within the flammability limit and sufficient heat source to ignite this mixture [41]. These conditions must be realized at the same time. Continual firebrand bombardment provided the heat source in these experiments to transition smoldering ignition to flaming ignition. Ohlemiller [41] reported that for wood to transition from

Figure 8. Picture of a cedar crevice where ignition was not observed. In this image, the cedar was oven dried, the wind tunnel speed was 6 m/s, and the firebrand generation rate was 0.01 g/s (based on a feed rate of 11.7 g/min).

Copyright © 2011 John Wiley & Sons, Ltd.

DOI: 10.1002/fam

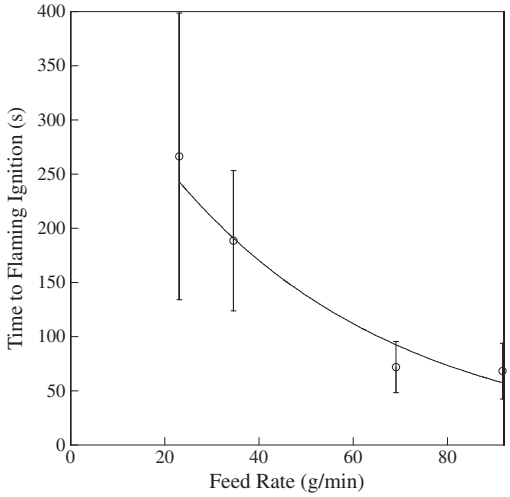

Figure 9. Time to flaming ignition (FI) as a function of feed rate for fixed wind tunnel speed when using dried cedar crevices.

smoldering ignition to flaming ignition, the wood must be arranged in a configuration to minimize heat losses, such as a crevice. Similar to the results reported in this study, Ohlemiller [41] found that wood transitioned consistently from smoldering ignition to flaming ignition in wood crevices but the time of this transition was varied and unpredictable. The study of the transition to flaming ignition from smoldering ignition has been studied experimentally and theoretically for some time and is still not well characterized because of the inherent complexity of the problem [e.g. 41–43]. Nevertheless, it is important to point that common building materials, such as cedar, were observed to transition to flaming ignition under continued firebrand bombardment. The onset of flaming ignition is clearly a very hazardous condition for structures located within the WUI.

4. COMPARISON TO PRIOR STUDIES

Although limited studies exist with respect to firebrand ignition of building materials, it is nonetheless useful to compare these detailed results to prior studies. Dowling [26] performed experiments to

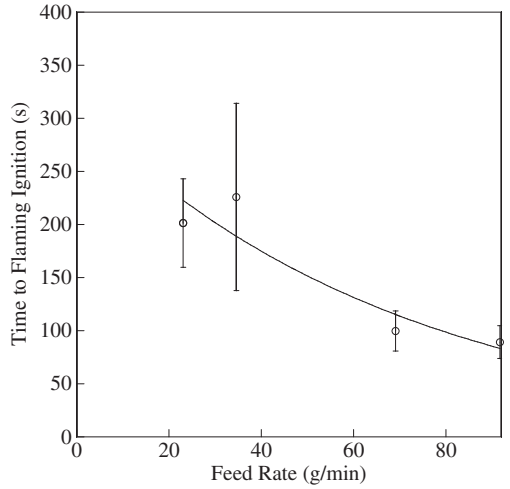

Figure 10. Time to flaming ignition (FI) as a function of feed rate for fixed wind tunnel speed when using moist cedar crevices.

Copyright © 2011 John Wiley & Sons, Ltd.

DOI: 10.1002/fam

Figure 11. Picture of flaming ignition of the cedar crevice. In this image, the cedar was oven dried, the wind tunnel speed was 6 m/s, and the firebrand generation rate was 0.14 g/s (based on a feed rate of 91.7 g/min).

investigate ignition of wood bridge members due to firebrand deposition. In these laboratory experiments, Dowling [26] burned wood cribs, and the resultant firebrands were collected and deposited into a 10 mm gap between the wood bridge members (deck plank and gravel beam). The mass of the firebrands (7 g to 35 g) generated was varied by altering the initial mass of the wood crib. The greater the wood crib mass, the greater the mass of the resultant firebrands. It was observed that 7 g of firebrands was able to produce smoldering ignition of the wood members within the 10 mm gap. The state of the firebrands upon deposition into 10 mm gaps, that is glowing or flaming, was not specified. Based on the present results, the mass of firebrands in the crevices used was in qualitative agreement with Dowling [26].

Prior to constructing the Dragon's LAIR, an experimental apparatus to investigate the ignition of fuel beds as a result of impact with burning firebrands was developed [29,38,44]. The apparatus allowed for the ignition and deposition of both single and multiple firebrands (only up to four) onto the target fuel bed and very limited applied flow velocities (up to 2.4 m/s). In that apparatus, four 50 mm glowing firebrands (mass = 4.5 g) were unable to produce ignition of dried cedar crevices (with applied wind up to 1.0 m/s). Naturally, moist cedar crevices did not ignite after contact with four glowing firebrands as well. Ignition was only observed for cedar crevices when flaming firebrands were deposited [44].

The influence of continually bombarding the cedar crevice with a dynamic firebrand flux is apparent from the present results. Under these conditions, it was quite easy to produce ignition, even when the cedar crevices were not dried. The new and improved Dragon's LAIR facility more accurately represents dynamic firebrand showers observed in real WUI fires.

Finally, it is instrumental to compare the results of this study to recent full-scale experiments using the NIST Dragon at the FRWTF. A full-scale reentrant corner, fitted with cedar shingle siding (the same cedar used for the present crevice experiments), was constructed for testing (each side was 122 cm wide by 244 cm high). An image of these experiments is shown in Figure 12. The moisture content of the cedar shingle siding at the time of testing was determined to be 11% and the wind tunnel speed was 7 m/s, similar conditions to the experiments described in this paper. Because it was not possible to dry the cedar shingle siding under full-scale experimental conditions, experiments were conducted by exposing the same reentrant corner assembly to repeat exposures using the NIST Dragon. The exposure time of firebrands from the NIST Dragon is 6 min, and it is possible to load the device and start a new experiment within 10 min of completing the prior test; therefore three exposure tests can be conducted relatively quickly. After the first exposure, essentially nothing was observed to happen because the moisture of the cedar was too high to produce smoldering ignition. It was observed that after the third exposure to firebrand showers, the cedar shingle siding ignited at the base of the wall assembly. These results qualitatively demonstrate that continual firebrand

Copyright © 2011 John Wiley & Sons, Ltd.

DOI: 10.1002/fam

Figure 12. Picture of cedar siding reentrant corner assembly under firebrand bombardment.

bombardment may produce smoldering ignition of moist cedar, even under full-scale applications. These experiments have demonstrated the need for a full-scale continuous firebrand generator.

5. SUMMARY

The present investigation was undertaken to construct a new and improved Dragon's LAIR facility. The unique feature of the continuous feed Baby Dragon, as opposed to the current NIST Baby Dragon, is the capability to produce a constant firebrand shower in order to expose building materials to continual firebrand bombardment. Ignition regime maps were determined as a function of glowing firebrand generation rate for fixed wind tunnel speed and two different moisture contents. For given moisture content and wind speed, the ignition delay time was observed to decrease as the firebrand generation rate was increased. The time to flaming ignition, after the onset of smoldering ignition, was also measured. As compared to the time required to reach smoldering ignition, the time to reach flaming ignition was less repeatable. This work has set the stage to be able to evaluate and compare various building materials' resistance to ignition from firebrand showers for the first time.

ACKNOWLEDGMENTS

The staff of the EL-NIST Large Fire Laboratory is acknowledged for their excellent assistance with the experimental campaign (Dr. Matthew F. Bundy—Supervisor; Mr. Laurean DeLauter, Mr. Anthony Chakalis, and Mrs. Doris Rinehart—Engineering Technicians). Mr. John R. Shields of EL-NIST is acknowledged for assisting in constructing the Firebrand Generator used for these experiments. Mr. Edward Hnetkovsky of EL-NIST is acknowledged for assisting in gate fabrication. The Science and Technology Directorate of the U.S. Department of Homeland Security sponsored the production of this material under Interagency Agreement IAA HSHQDZ-10-X-00288 with the National Institute of Standards and Technology (NIST).

REFERENCES

1. Maranghides A, Mell WE. A case study of a community affected by the Witch and Guejito fires. *Fire Technology* 2011; **47**:379–420.
2. Blanchi R, Leonard JE, Leicester RH. Lessons learnt from post-fire surveys at the urban interface in Australia. *Proceedings of the Fifth International Conference on Forest Fire Research*, Figueria da Foz, Portugal, 2006.

Copyright © 2011 John Wiley & Sons, Ltd.

DOI: 10.1002/fam

3. Cohen JD, Stratton J. Home destruction examination, Grass Valley Fire, Lake Arrowhead, CA. *USDA Report R5-TP-026 b*, 2008.
4. Wilson AAG, Ferguson IS. Predicting the probability of house survival during bushfires. *Journal of Environmental Management* 1986; **23**:259–270.
5. Ramsay GC, McArthur NA, Dowling VP. Building survival in bushfires. *Fire Science 186: The 4th Australian National Biennial Conference*, 1986; 17.
6. Abt R, Kelly D, Kuypers M. The Florida Palm Coast fire: an analysis of fire incidence and residence characteristics. *Fire Technology* 1987; **23**:186–197.
7. Gordon DA. Structure survival in the urban/wildland interface: a logistic regression analysis of the Oakland/Berkeley tunnel fire. *MS Thesis*, University of California at Berkeley, 2000; 447.
8. Foote EID. Structure survival on the 1990 Santa Barbara "Paint" fire: a retrospective study of urban-wildland interface fire hazard mitigation factors. *MS Thesis*, University of California at Berkeley, 1994; 129.
9. McArthur NA, Lutton P. Ignition of exterior building details in bushfires: an experimental study. *Fire and Materials* 1991; **1**:59–64.
10. Foote EID, Martin R, Gilless JK. The defensible space factor study: a survey instrument for post-fire structure loss. *Conference Proceedings, 11th Conference on Fire and Forest Meteorology*, Society of American Foresters, 1991; 8.
11. Albini F. Spot fire distances from burning trees—a predictive model. *USDA Forest Service General Technical Report INT-56*, Missoula, MT, 1979.
12. Albini F. Transport of firebrands by line thermals. *Combustion Science and Technology* 1983; **32**:277–288.
13. Muraszew A, Fedele JF. Statistical model for spot fire spread. *The Aerospace Corporation Report No. ATR-77758801*, Los Angeles, CA, 1976.
14. Tarifa CS, del Notario PP, Moreno FG. On the flight paths and lifetimes of burning particles of wood. *Proceedings of the Combustion Institute* 1965; **10**:1021–1037.
15. Tarifa CS, del Notario PP, Moreno FG. Transport and combustion of fire brands. Instituto Nacional de Tecnica Aerospacial "Esteban Terradas". *Final Report of Grants FG-SP 114 and FG-SP-146*, vol. 2 (Madrid, Spain), 1967.
16. Tse SD, Fernandez-Pello AC. On the flight paths of metal particles and embers generated by power lines in high winds and their potential to initiate wildfires. *Fire Safety Journal* 1998; **30**:333–356.
17. Anthenian R, Tse SD, Fernandez-Pello AC. On the trajectories of embers initially elevated or lofted by small scale ground fire plumes in high winds. *Fire Safety Journal* 2006; **41**:349–363.
18. Woycheese JP. Brand lofting and propagation for large-scale fires. *Ph.D. Thesis*, University of California, Berkeley, 2000.
19. Himoto K, Tanaka T. Transport of disk-shaped firebrands in a turbulent boundary layer. In Fire Safety Science—Proceedings of the Eighth International Symposium, Gottuk D, Lattimer B (eds). International Association of Fire Safety Science (IAFSS): London, 2005; 433–444.
20. Knight IK. The design and construction of a vertical wind tunnel for the study of untethered firebrands in flight. *Fire Technology* 2001; **37**:87–100.
21. Wang HH. Analysis of downwind distribution of firebrands sourced from a wildland fire. *Fire Technology* 2011; **47**:321–340.
22. Waterman TE. Experimental study of firebrand generation. IIT Research Institute, Project J6130, Chicago, IL, 1969.
23. Manzello SL, Maranghides A, Mell WE. Firebrand generation from burning vegetation. *International Journal of Wildland Fire* 2007; **16**:458–462.
24. Manzello SL, *et al*. Mass and size distribution of firebrands generated from burning Korean pine (*Pinus koraiensis*) trees. *Fire and Materials* 2009; **33**:21–31.
25. Waterman TE, Takata AE. Laboratory study of ignition of host materials by firebrands. Project J-6142-OCD Work Unit 2539A, IIT Research Institute, Chicago, IL, 1969.
26. Dowling VP. Ignition of timber bridges in bushfires. *Fire Safety Journal* 1994; **22**:145–168.
27. Ellis PF. The aerodynamic and combustion characteristics of eucalypt bank—a firebrand study. *Ph.D. Dissertation*, Australian National University, Canberra, 2000.
28. Ganteaume A, Lampin-Maillet C, Guijarro M, Hernando C, Jappiot M, Fonturbel T, Perez-Gorostiaga P, Vega JA. Spot fires: fuel bed flammability and capability of firebrands to ignite fuel beds. *International Journal of Wildland Fire* 2009; **18**(8):951–969.
29. Manzello SL, Cleary TG, Shields JR, Yang JC. Ignition of mulch and grasses by firebrands in wildland–urban interface (WUI) fires. *International Journal of Wildland Fire* 2006; **15**:427–431.
30. Manzello SL, Shields JR, Yang JC, Hayashi Y, Nii D. On the use of a firebrand generator to investigate the ignition of structures in WUI fires. *Proceedings of the 11th International Conference on Fire Science and Engineering (INTERLFAM)*, Interscience Communications, London, 2007; 861–872.
31. Manzello SL, Shields JR, Hayashi Y, Nii D. Investigating the vulnerabilities of structures to ignition from a firebrand attack. In Fire Safety Science—Proceedings of the Ninth International Symposium, Karlsson B (ed.), vol. **9**, International Association of Fire Safety Science (IAFSS): London, 2008; 143–154.
32. Manzello SL, Hayashi Y, Yoneki Y, Yamamoto Y. Quantifying the vulnerabilities of ceramic tile roofing assemblies to ignition during a firebrand attack. *Fire Safety Journal* 2010; **45**:35–43.
33. Manzello SL, Park SH, Shields JR, Hayashi Y, Suzuki S. Comparison testing protocol for firebrand penetration through building vents: summary of BRI/NIST full scale and NIST reduced scale results, NIST TN 1659, January, 2010.

Copyright © 2011 John Wiley & Sons, Ltd.

DOI: 10.1002/fam

34. Manzello SL, Park SH, Suzuki S, Shields JR, Hayashi Y. Experimental investigation of structure vulnerabilities to firebrand showers. *Fire Safety Journal* 2011; doi: 10.1016/j.firesafe.2011.09.003.
35. Suzuki S, Manzello SL. On the development and characterization of a reduced scale continuous feed firebrand generator. In Fire Safety Science—Proceedings of the Tenth International Symposium, Spearpoint M (ed.), vol. **10**, International Association of Fire Safety Science (IAFSS): London, 2011; in press.
36. Foote EID, Liu J, Manzello SL. Characterizing firebrand exposure during wildland-urban interface fires. *Proceedings of Fire and Materials 2011 Conference*, Interscience Communications, London, 2011; 479–492.
37. ASTM E108. Fire Standards and Flammability Standards. ASTM International: West Conshohocken, PA, 2003; doi: 10.1520/E0108-10A, www.astm.org.
38. Manzello SL, Park SH, Cleary TG. Investigation on the ability of glowing firebrands deposited within crevices to ignite common building materials. *Fire Safety Journal* 2009; **44**:894–900.
39. North GA. An analytical model for vertical flame spread on solids: an initial investigation. *Fire Engineering Research Report 99/12*, School of Engineering, Univ. Canterbury, Christchurch, New Zealand, 1999.
40. Tewarson T. Generation of Heat and Chemical Compounds in Fires. SFPE Handbook of Fire Protection Engineering (2nd edn). NFPA: Quincy, Mass., USA, 1992; 3–53.
41. Ohlemiller T. Smoldering combustion propagation on solid wood. In Fire Safety Science—Proceedings of the Third International Symposium, Cox G (ed.), vol. **3** International Association of Fire Safety Science (IAFSS). Elsevier: London, 1991; 565.
42. Tse SD, Fernandez-Pello AC, Miyasaka K. Controlling mechanisms in the transition from smoldering to flaming of flexible polyurethane foam. *Proceedings of the Combustion Institute* 1996; **26**:1505–1513.
43. Aldushin AP, Bayliss A, Matkowsky BJ. On the transition from smoldering to flaming. *Combustion and Flame* 2006; **145**:579–606.
44. Manzello SL, Cleary TG, Shields JR, Yang JC. On the ignition of fuel beds by firebrands. *Fire and Materials* 2006; **30**:77–87.

Copyright © 2011 John Wiley & Sons, Ltd.

DOI: 10.1002/fam